frontiers | Frontiers in Energy Research

TYPE Original Research
PUBLISHED 29 August 2022
DOI 10.3389/fenrg.2022.973336

OPEN ACCESS

EDITED BY
Yongjin Fang,
City University of Hong Kong, Hong Kong SAR, China

REVIEWED BY
Zhongxue Chen,
Wuhan University, China
Min Zhou,
Huazhong University of Science and Technology, China

*CORRESPONDENCE
Lan Xia,
xialan@nbu.edu.cn

SPECIALTY SECTION
This article was submitted to Electrochemical Energy Conversion and Storage,
a section of the journal
Frontiers in Energy Research

RECEIVED 20 June 2022
ACCEPTED 01 August 2022
PUBLISHED 29 August 2022

CITATION
Chen M, Liu Z, Zhao X, Li K, Wang K, Liu Z, Xia L, Yuan J and Zhao R (2022), Fluorinated co-solvent electrolytes for high-voltage Ni-rich $LiNi_{0.8}Co_{0.1}Mn_{0.1}O_2$ (NCM811) positive electrodes.
Front. Energy Res. 10:973336.
doi: 10.3389/fenrg.2022.973336

Fluorinated co-solvent electrolytes for high-voltage Ni-rich $LiNi_{0.8}Co_{0.1}Mn_{0.1}O_2$ (NCM811) positive electrodes

Mingming Chen[1], Zezhao Liu[1], Xinzhe Zhao[1], Kuihao Li[1], Kehuang Wang[1], Zhishan Liu[1], Lan Xia[1]*, Jinliang Yuan[1] and Ruirui Zhao[2]

[1]Faculty of Maritime and Transportation, Ningbo University, Ningbo, China, [2]EVE Energy Co., Ltd., HuiZhou, China

Nickel-rich $LiNi_{0.8}Co_{0.1}Mn_{0.1}O_2$ (NCM811) is one of the most promising positive electrodes for utilization in the next-generation of lithium-ion batteries. Charging the NCM cells above 4.3 V is proposed to be beneficial for its reversible capacity. However, the high reactivity of the NCM811 usually results in parasitic electrolyte degradation, which is accelerated with the increase of the Ni content in the NCM positive electrodes, leading to the thickening of the positive electrode-electrolyte interphase during cycling. Herein, to counter this issue, we select partially fluorinated solvents, such as methyl 3,3,3-trifluoropropanoate (MTFP) and 1,1,1,2,2,3,3,4,4-nonafluoro-4-methoxybutane (NFMB), as a co-solvent for fluoroethylene carbonate (FEC)-based electrolytes, and detailed investigate theirs physical, chemical, and electrochemical properties for applications in NCM811 materials. Compared to the carbonate-based electrolyte without a fluorinated solvent, the electrolytes with a fluorinated co-solvent display an obviously enhanced cycling performance of the Li/NCM811 cells charged to above 4.5 V. This work suggests that fluorinated co-solvent electrolytes provide an alternative way to the high-concentration electrolyte for the design of new electrolyte systems for high energy density lithium-ion batteries.

KEYWORDS

lithium-ion battery, high energy density, LiNi0.8Co0.1Mn0.1O2, electrolyte, fluorinated solvent, interphase

Introduction

Electrochemical energy storages are the most important form of energy storages. Nowadays, lithium-ion batteries (LIBs) are the important power sources for portable electronics, electric vehicles, aerospace, and deep-sea diving devices due to their high energy density, acceptable cycle life, and no memory effect (Wang et al., 2020; He et al., 2021). With the continuous expansion of the application fields of LIBs, lots of efforts have been made to further improve their energy density and safety (Leach et al., 2022; Li et al.,

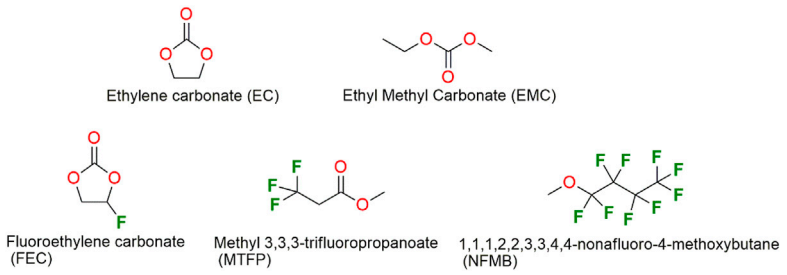

SCHEME 1
Molecular structures of all solvents used in this work.

2022; Yang et al., 2022). So far, Nickel-rich $LiNi_xCo_yMn_{1-x-y}O_2$ (NCM for short, x ≥ 0.6) materials, specially, Nickel-rich $LiNi_{0.8}Co_{0.1}Mn_{0.1}O_2$ (NCM811 for short) positive electrodes are one of the most promising positive electrodes for utilization in the next-generation of lithium-ion batteries (Li et al., 2020; Xue et al., 2021). The theoretical capacity of NCM811 can reach 278 mAh g^{-1}, but its practical capacity is only 130–200 mAh g^{-1}, which is mainly due to the limited cyclability of NCM811 battery at a cut-off voltage of >4.3 V (Xu et al., 2020; Fan and Wang, 2021; Niu et al., 2021; Zhang et al., 2021). Noted that the reversible capacity of the NCM811 is positively associated with the charging cut-off voltage (Chen et al., 2017). Charging the NCM batteries above 4.3 V is proposed to be advantageous to its reversible capacity. Thus, increasing the charging cut-off voltage is an attractive approach to further improve the reversible capacity of the NCM811 positive electrodes. However, because of the poor stability against oxidation of conventional carbonate-based electrolytes above 4.3 V *vs.* Li^+/Li, it is now well recognized that the high reactivity of the NCM811 usually results in parasitic electrolyte degradation, which is accelerated with the increase of the Ni content in the NCM positive electrodes, leading to the thickening of the positive electrode-electrolyte interphase upon cycling (Li et al., 2015; Ryu et al., 2018). Some strategies, including surface coating with the oxide layer (Schipper et al., 2017; Huang et al., 2019), designing concentration-gradient structures (Park et al., 2015; Lim et al., 2016), utilizing functional electrolyte additives (Li et al., 2017; Lan et al., 2019; Liu et al., 2019; Lim et al., 2020; Gu et al., 2022), and employing anti-oxidative electrolytes (Cao et al., 2019a; Heist et al., 2019; Liu et al., 2022), have been proposed to enhance the interfacial stability of the NCM electrodes. Among these strategies, electrolyte engineering is thought to be one of the most effective and feasible approaches to stabilize the interface between the electrode and the electrolyte.

The fluorinated solvent-containing electrolytes, with high electrochemical stability, are valuable options for nickel-rich NCM811 positive electrodes under this background (Fan et al., 2018; Xia et al., 2021; Pham et al., 2019; Cao et al., 2019a; Lee et al., 2019; Zhu et al., 2022]. For instance, Pham et al. (Pham et al., 2019) have reported highly stable cycling of Li/NCM811 cells up to 100 cycles with a capacity retention of 95% by charging to 4.5 V in a non-flammable electrolyte of propylene carbonate (PC) and fluorinated linear carbonates. Unfortunately, the good performance has been gained with low current density (0.2C), which may due to its high viscosity. Introducing low-viscosity cosolvents into highly concentrated electrolytes has been proven as a feasible route to reduce viscosity and obtain good compatibility toward 4 V-calss Ni-rich positive electrodes (Cao et al., 2019b; Lee et al., 2019). Meanwhile, the fluorinated aromatic diluents pairing with anions has been proposed as a new class of cosolvents for high-concentration electrolytes of consisting of a mixture of lithium bis(fluorosulfonyl)imide (LiFSI), 1,2-dimethoxyethane (DME) (Zhu et al., 2022). This, the anion-diluent pairing's improved compatibility with the reactive Ni-rich electrodes, enables an 80% capacity retention of a 20 μm thin Li/high-loading-NCM811 (3.5 mAh cm^{-2}) cell for 260 cycles at a cut-off charging voltage of 4.3 V. Not long ago, 1,1,2,2-tetrafluoroethyl-2,2,3,3-tetrafluoropropyl ether (TTE) has also been demonstrated as an inert cosolvent to develop a nonflammable low concentration electrolyte for Graphite/NCM523 pouch cells (Guan et al., 2022). This case casts a new insight into the development of LIB electrolytes. Although progresses have been made in stabilizing fluorinated interphases through fluorinated co-solvents, studies on enabling the cycling of NCM811 at a high cut-off charging voltage of above 4.5 V are still rare.

In our previous work (Xia et al., 2021), we found that the partially fluorinated ethers, such as 1,1,1,3,3,3-hexafluoroisopropyl methyl ether (HFPM) and 1,1,2,2-tetrafluoroethyl-2,2,3,3-tetrafluoropropyl ether (TTE), as a co-solvent of fluoroethylene carbonate (FEC)-based electrolytes, demonstrated an obviously improved cycling and rate properties of the Li/NCM811 cells cycled between 2.7 and 4.3 V. However, these two cosolvents cannot improve the cycling of NCM811 at a high cut-off charging voltage of

above 4.5 V. Therefore, in this work, we select partially fluorinated solvents, including methyl 3,3,3-trifluoropropanoate (MTFP) and 1,1,1,2,2,3,3,4,4-nonafluoro-4-methoxybutane (NFMB), as a co-solvent for fluoroethylene carbonate (FEC)-based electrolytes to suppress the electrolyte decomposition during NCM811 cycling stability at high voltage operation. Scheme 1 displays the molecular structures of all used solvents. We systematically investigate their electrochemical properties for applications in NCM811 electrode materials. Compared to the carbonate-based electrolyte without a fluorinated solvent, the electrolytes with a fluorinated co-solvent displays an obviously enhanced cycling performance of the Li/NCM811 cells charged to 4.7 and 4.8 V.

Materials and methods

Materials

High energy density positive electrode materials-single crystal Nickel-rich $LiNi_{0.8}Co_{0.1}Mn_{0.1}O_2$ (NCM811) powders, super carbon black powders, N-methyl pyrrolidone (NMP, purity: ≥99.5%) and polyvinylidene difluoride (PVDF, purity: ≥99.5%) were purchased from Shenzhen Kejing Zhida Technology Co., Ltd. Lithium battery grade solvents including ethylene carbonate (EC, purity: ≥ 99.5%) and ethyl methyl carbonate (EMC, purity: ≥ 99.5%) and lithium salt $LiPF_6$, were purchased from Shanghai Yongchuan Biological Co., Ltd. Fluorinated solvents, such as methyl 3,3,3-trifluoropropanoate (MTFP, purity ≥97%), 1,1,1,2,2,3,3,4,4-nonafluoro-4-methoxybutane (NFMB, purity: ≥ 99%) and fluoroethylene carbonate (FEC) were also purchased from Shanghai Yongchuan Biological Co., Ltd. Lithium sheets (purity: ≥ 99%) were purchased from China Energy Lithium Co., Ltd. All these materials were used without any measurements.

Preparation of electrolytes and electrodes

All the electrolyte solutions were prepared in a glove-box filled with high purity argon (purity: 99.99%). First, we prepared the FEC-based electrolyte of 1 mol L^{-1} (M) $LiPF_6$ EMC-FEC (6:1, v/v). Then, we added some fluorinated solvent into the above-mentioned FEC-based electrolyte, and obtained the electrolytes of 1 M $LiPF_6$ MTFP/EMC/FEC (3:6:1, v/v/v) and 1 M $LiPF_6$ NFMB/EMC/FEC (3:6:1, v/v/v). For comparison, the conventional EC-based electrolyte was composed of 1.0 mol L^{-1} $LiPF_6$ dissolved in the mixture solvent of EMC and EC in a 6:1 volume ratio (noted as 1 M $LiPF_6$ EMC/EC). The electrodes were prepared by using 80 wt% NCM811 positive electrode materials as active materials, 10 wt% super P carbon black powders as conductive materials and 10 wt% polyvinylidene fluoride as binders. The obtained uniform NCM811 slurry was casted on an aluminum foil with a thickness of 25 μm by the scraper method. And then the obtained electrodes were dried in a vacuum drying oven at 120°C for 12 h. After drying, the MSK-T10 manual punch was used to punch out the NCM811 electrode sheets with diameter 12 mm. Before assembling into CR2032 coin-cells, all the electrode sheets were dried at 60°C for 6 h again.

Electrochemical tests and characterization techniques

Their ionic conductivities were measured on a DDSJ-319L conductivity meter (Shanghai INESA Scientific instrument Co., Ltd.) in the temperature range from −40 to 60°C. To test the chemical stability of pure solvents with Li sheet, we took Li metal sheet immersing in the pure solvent in an Ar-filled glove box. Then, we collected the corresponding picture after placed for 0, 6 and 24 h. The oxidative stabilities of the prepared electrolytes were obtained by cyclic voltammetry (CV), which used stainless steel symmetrical CR2032-type coin-cells using a CHI660e electrochemical workstation (Shanghai Chenhua instrument Co., Ltd.) at a scanning speed of 0.1 mV s^{-1}. The battery charge and discharge tests were carried out on the computer-controlled battery charger (LANDCT 3002A land battery test system, Wuhan, China). The current density was 40 mA g^{-1}, and the charge/discharge voltage range was 2.7–4.5 V. In order to obtain the rate properties of Li/NCM811 coin-cells with different electrolytes, the rate charge-discharge tests were carried out at a current density of 20 mA g^{-1} (C/8), 40 mA g^{-1} (C/4), 80 mA g^{-1} (C/2), 160 mA g^{-1} (1C), 320 mA g^{-1} (2C) and 640 mA g^{-1} (4C). To investigate the high-voltage cycle performance of fluorine-containing electrolytes at a high cut-off voltage of >4.5 V, the electrochemical performance of NCM811 cells charged to 4.7 and 4.8 V was measured at a current density of 40 mA g^{-1}. The graphite/$LiCoO_2$ pouch cells (Type: 401824, 265 mAh, balanced for 4.45 V) without electrolyte were fabricated by EVE Energy Co., Ltd. These cells without drying treatment were transferred into the argon-filled glove-box. And then, the electrolyte was injected into the pouch cell that was then sealed. The formation process and electrochemical tests were measured by the LANDCT 3002K-1A land battery test system. The formation process was as follows: the cells in this study were charged with the current of 53 mA for 30 min with a cut-off voltage of 3.4 V, and the constant current charging process was carried out for 70 min at 185.5 mA with the cut-off voltage of 4.1 V and the cut-off current of 13.25 mA. After the formation steps, the pouch cells were charged and discharged at 53 mA (0.2 C) between 2.7 and 4.5 V with the constant-current constant-voltage (CC–CV) protocol at room temperature. The cut-off current for CC-CV protocol was 0.02 C. The low-temperature performance of the coin-cells was tested in high-low temperature test chamber.

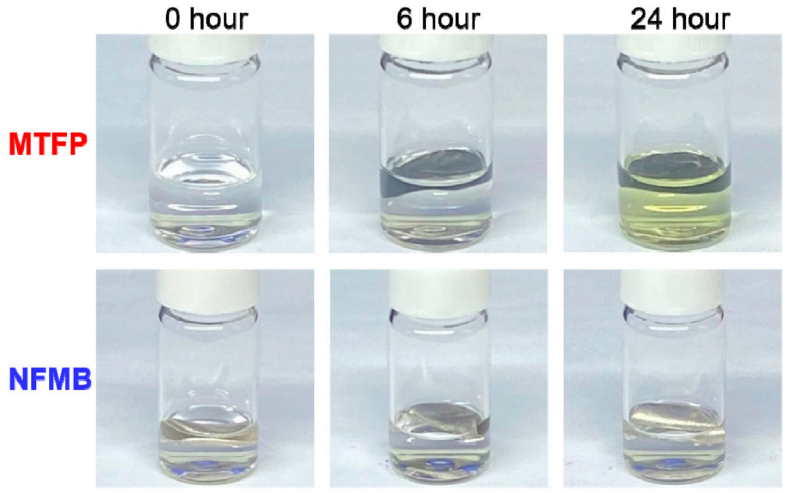

FIGURE 1
Reactivity of lithium metal sheet and pure solvents at room temperature.

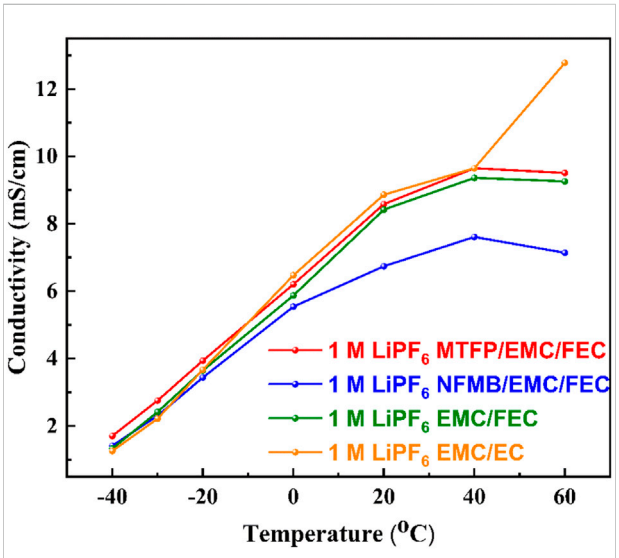

FIGURE 2
Ionic conductivity of different electrolytes in the temperature range of −40–60°C.

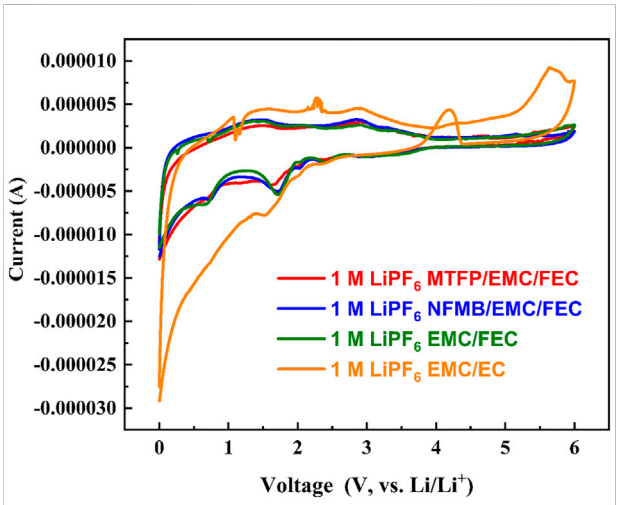

FIGURE 3
Cyclic voltammetry curves of electrolytes at a scan rate of 0.1 mV s^{-1} at 25°C on Li/SS coin cells.

Scanning electron microscopy (SEM) tests were measured on the surface of NCM811 electrodes before and after cycled. For SEM measurements, the NCM811/Li coin-cells were cycled and disassembled in a glove box. The NCM electrodes were directly collected without pure DMC washing. The electrochemical impedance spectroscopy (EIS) was carried out on the CHI660e electrochemical workstation (Shanghai Chenhua instrument Co., Ltd.). The EIS measurements in the frequency range of 100 kHz~100 mHz were performed with an oscillation amplitude of 5 mV.

Results and discussion

All the prepared electrolytes are transparent, colorless liquids. In order to study the reactivity of Li metal with the pure solvent at room temperature, we did a series of chemical stability experiments. The change trend of the chemical stability of pure solvents with storage time can be visually observed by immersing Li sheets into the pure solvent. Figure 1 shows the photos of these pure solvents and Li sheets after storage for 0, 6 and 24 h, respectively. After 24 h, for MTFP, its color becomes light yellow, which may be due to the reaction between the MTFP

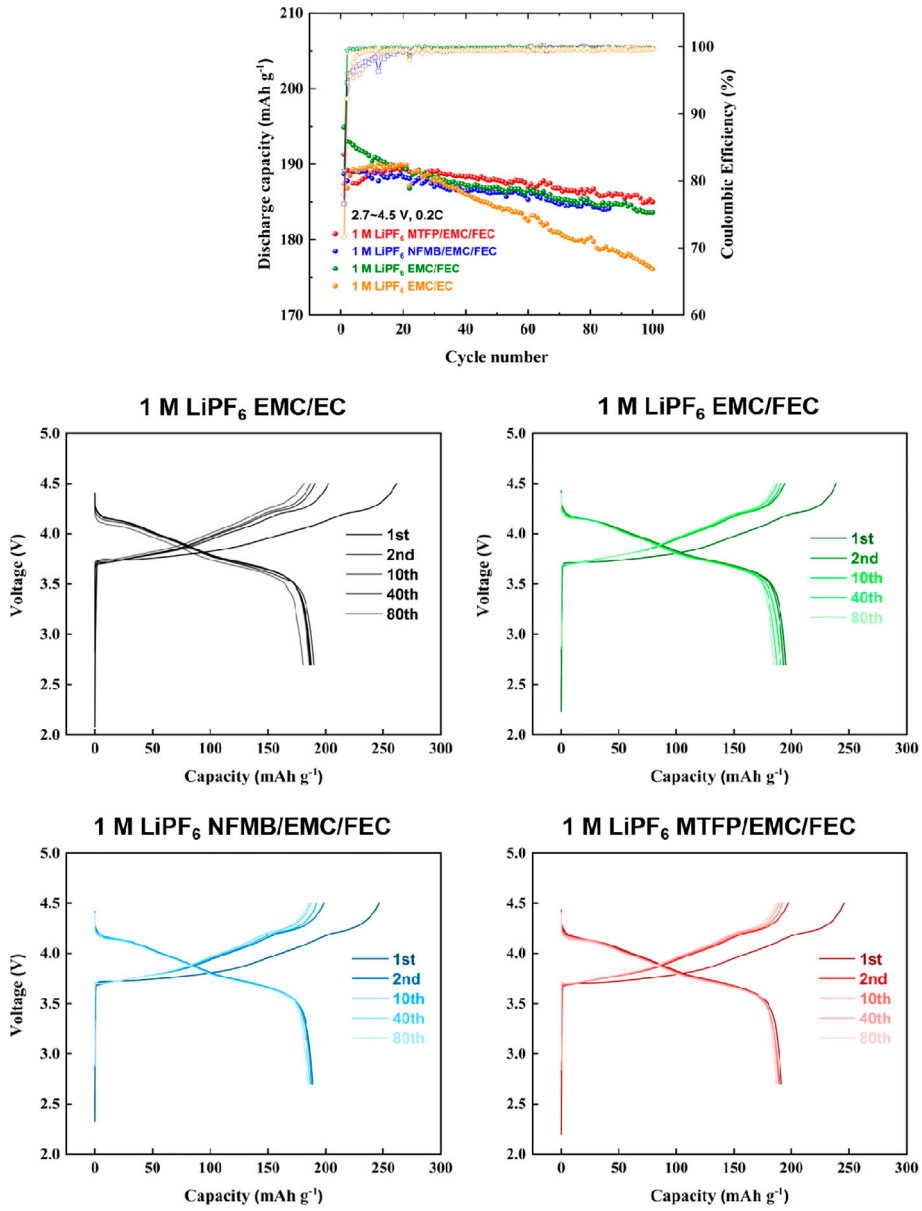

FIGURE 4
Charge-discharge cycling performances of Li/NCM811 coin-cells assembled with different electrolytes at a cut-off voltage of 2.7–4.5 V and a current density of 0.2 C.

and Li metal. However, in pure NFMB, there is still no obvious color change for Li sheet and the solvent even after 24 h. Such an experimental phenomenon demonstrates that the NFMB can form stable SEI film on Li metal, which may be beneficial to the long-term cyclic stability of these solvent-containing electrolytes for lithium-ion batteries.

Figure 2 shows the ionic conductivities of two fluorinated cosolvent-containing electrolytes (1 M $LiPF_6$ MTFP/EMC/FEC and 1 M $LiPF_6$ NFMB/EMC/FEC), two control electrolytes (1 M $LiPF_6$ EMC/FEC and 1 M $LiPF_6$ EMC/EC). The conductivity of all these electrolytes has been found to increase with an increase in the temperature. However, at 60°C, the ionic conductivity of the electrolytes containing fluorinated solvents has been found to slightly decrease, which may be due to the decomposition of the FEC-containing electrolytes at 60°C. The introduction of NFMB into the 1 M $LiPF_6$ EMC/FEC electrolyte reduces the ionic conductivity of this electrolyte. However, compared to the 1 M $LiPF_6$ EMC/FEC electrolyte, MTFP with the carboxylic ester group can be beneficial to dissolve lithium salt, thus slightly increasing the conductivity of the 1 M $LiPF_6$ MTFP/

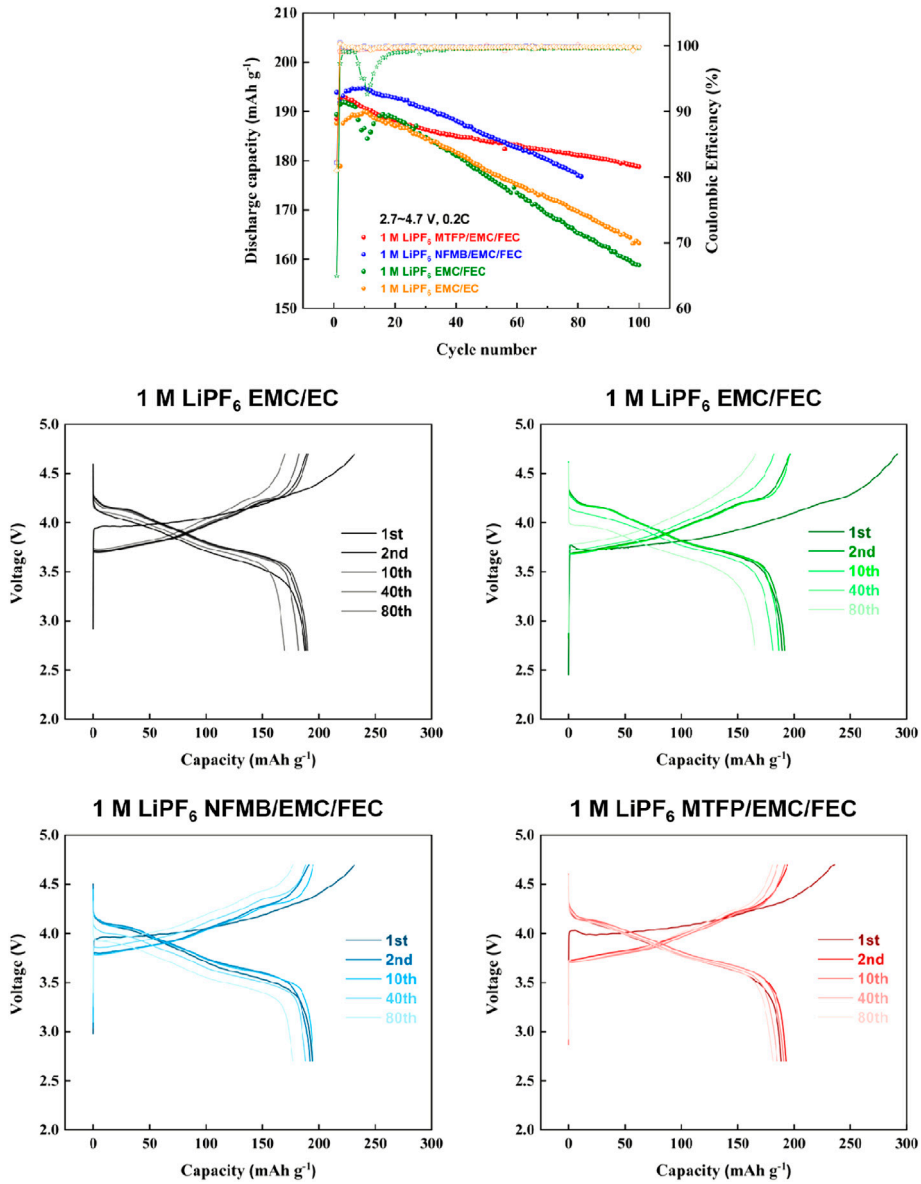

FIGURE 5
Charge-discharge cycling performances of Li/NCM811 coin-cells assembled with different electrolytes at a cut-off voltage of 2.7–4.7 V and a current density of 0.2 C.

EMC/FEC electrolyte in the temperature range of −40–60°C. Even at the low temperature of −40°C, the conductivity of the 1 M $LiPF_6$ MTFP/EMC/FEC electrolyte is 1.709 mS cm^{-1}, which is slightly higher than that of the EC-based electrolyte (1.264 mS cm^{-1}), and beneficial to its ion transport below −40°C.

In order to test the electrochemical voltage window of all the prepared electrolytes, cyclic voltammetry (CV) measurements were carried out. Figure 3 displays the cyclic voltammetry curves of Li sheet/stainless steel (Li/SS) CR2032 coin-cells containing different electrolytes in a voltage range of 0–6 V on CHI660e electrochemical workstation. The scanning speed is 0.1 mV s^{-1}. The Li/SS cells using the EC-based electrolyte experience significantly increased oxidation peaks above 4.1 V. Other three cells with fluorinated solvent-containing electrolytes show similar CV curves. Compared to the EC-based electrolyte, the oxidation stabilities of these fluorinated solvent-containing electrolytes were significantly improved, no obvious increase in oxidation current were observed until 6 V, which demonstrated an enhanced antioxidation stability and favored high-voltage positive electrodes. This result is mainly

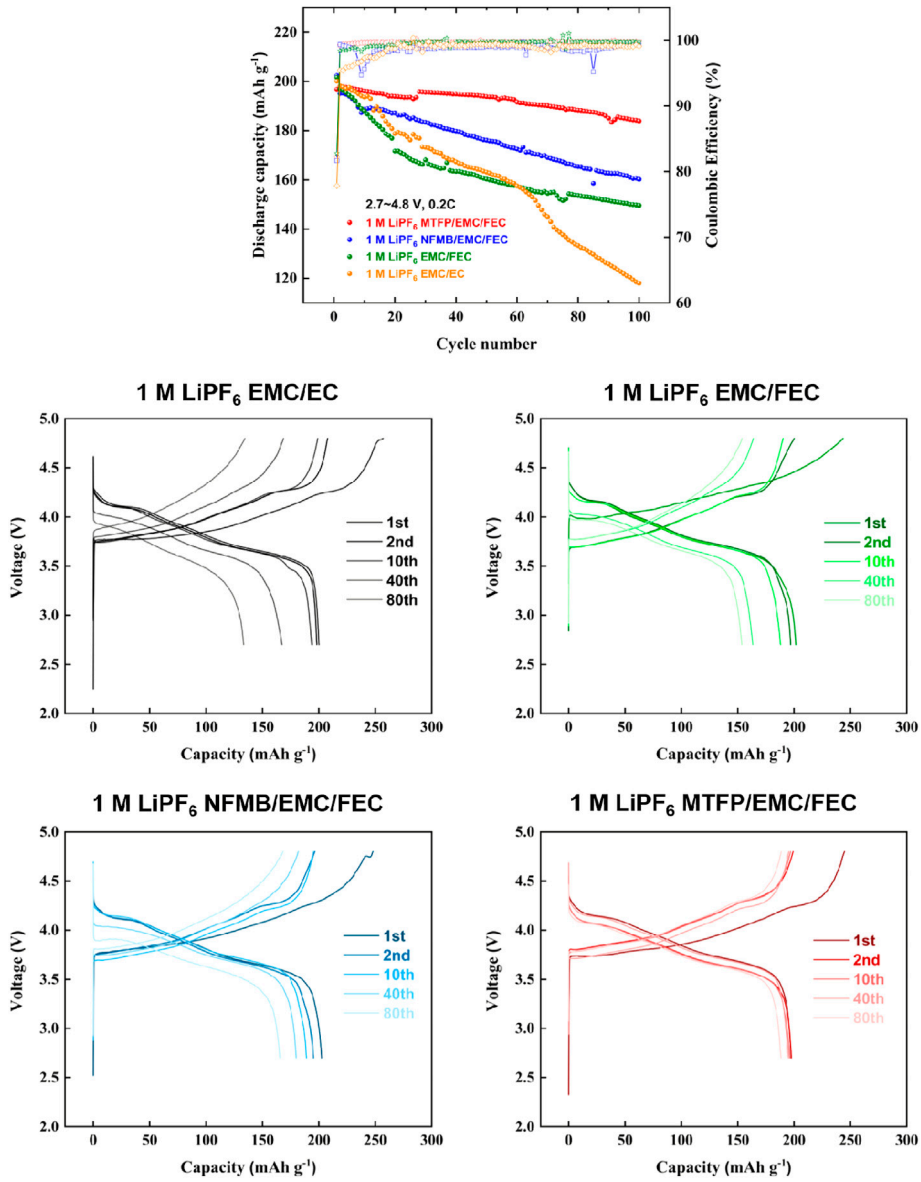

FIGURE 6
Charge-discharge cycling performances of Li/NCM811 coin-cells assembled with different electrolytes at a cut-off voltage of 2.7–4.8 V and a current density of 0.2 C.

due to the strong electro-negativity and weak polarity of fluorine atoms, the use of fluorine-containing solvent can effectively increase the oxidation decomposition voltage of the electrolyte, and thus the fluorine-containing cosolvent electrolyte can more easily meet the requirement of high-voltage electrolytes.

Figure 4 shows the comparison of the cycling properties of the Li/NCM811 cells cycled between 2.7 and 4.5 V with different electrolytes. As shown in Figure 4, in 1 M $LiPF_6$ EC/EMC electrolyte, the discharge capacity fades very rapidly with just 93.1% capacity retention after 100 cycles, which may be due to the instability interface. However, in other three electrolytes, significantly improved cycling performances are achieved. All the cells were stably cycled to the cut-off voltages of 4.5 V. As seen in the charge-discharge profiles, the cells assembled with 1 M $LiPF_6$ MTFP/EMC/FEC and 1 M $LiPF_6$ NFMB/EMC/FEC show similar charge-discharge curves, and a highly reversible charge-discharge behavior.

Fluorinated co-solvents of MTFP and NFMB are anticipated to promote high-voltage cycling performances of the NCM811 positive electrodes. In order to obtain higher voltage cycling performance, cycling tests of the cells at 2.7–4.7 V and

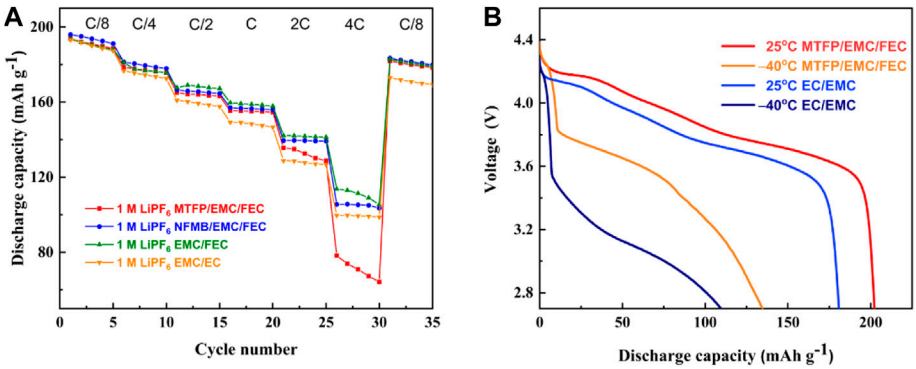

FIGURE 7
(A): Rate capability of Li/NCM811 coin-cells assembled with different electrolytes at the rate from C/8 to 4 C; **(B)**: Discharge curves of the coin-cells at 25 and –40°C with the current of 0.2 C.

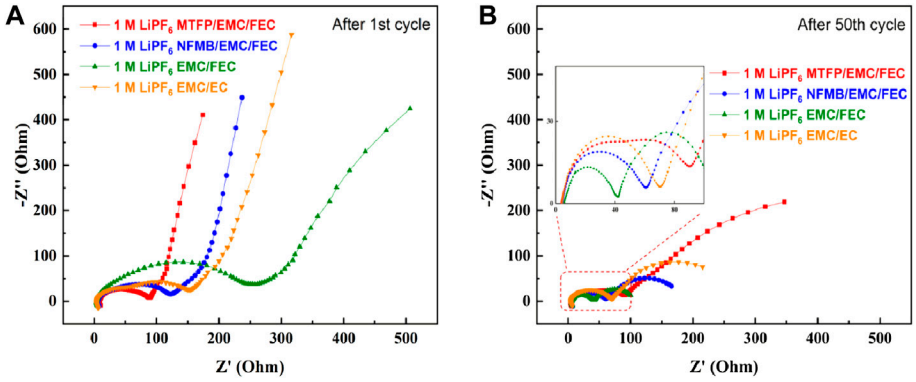

FIGURE 8
EIS tests of Li/NCM811 coin-cells assembled with different electrolytes at discharged to 3.0 V, **(A)** after 1 cycle; **(B)** after 50 cycles.

2.7–4.8 V were also measured as shown in Figures 5, 6. Once increasing the charge cut-off voltage to 4.7 and 4.8 V in the 1 M $LiPF_6$ EMC/EC and 1 M $LiPF_6$ EMC/FEC, the capacities of the cells faded very quickly, which showed that these two electrolytes did not satisfy the high-voltage cycling requirements of the NCM811 electrodes. Noted that for the 1 M LiPF6 EMC/EC, the capacity faded very quickly leading to just 59.7% capacity retention after 100 cycles. However, the cells with 1 M $LiPF_6$ MTFP/EMC/FEC and 1 M $LiPF_6$ NFMB/EMC/FEC showed good high-voltage cycling performances along with a discharge capacity is about 181.1 mAh g^{-1} and 177 mAh g^{-1} after 80 cycles, that is 96.1 and 91.3%, respectively. Moreover, when even charged to 4.8 V as shown in Figure 6, the NCM811 cells with 1 M $LiPF_6$ MTFP/EMC/FEC still showed excellent performance. After 100 cycles, the discharge capacity still reached to 183.9 mAh g^{-1}, that is, 93.2% capacity retention of its capacity of second cycle. These improved high voltage cycling performances may be attributed to their highly oxidative stability and very good LiF-rich interphase layers on the two electrodes (Fan et al., 2019). Unfortunately, the discharge capacity and capacity retention of the cells with 1 M $LiPF_6$ NFMB/EMC/FEC were 160.2 mAh g^{-1} and 81.2%, respectively, which were still much better than those of cells in the control group electrolytes. The reason was that the MTFP could form a more stable interface on the surface of the NCM811 positive electrodes, inhibiting the further parasitic reaction between the electrolyte and the positive electrode, and thus improving the high voltage cycle performance of the battery. These data showed that our prepared electrolytes caused the improvement of the high-voltage stability of the NCM811 electrode.

Figure 7A compares rate capability of Li/NCM811 coin-cells assembled with different electrolytes at the rate from C/8 to 4 C at room temperature and in the voltage range of 2.7–4.5 V. We observe that the cells with the EC-based electrolyte delivers a

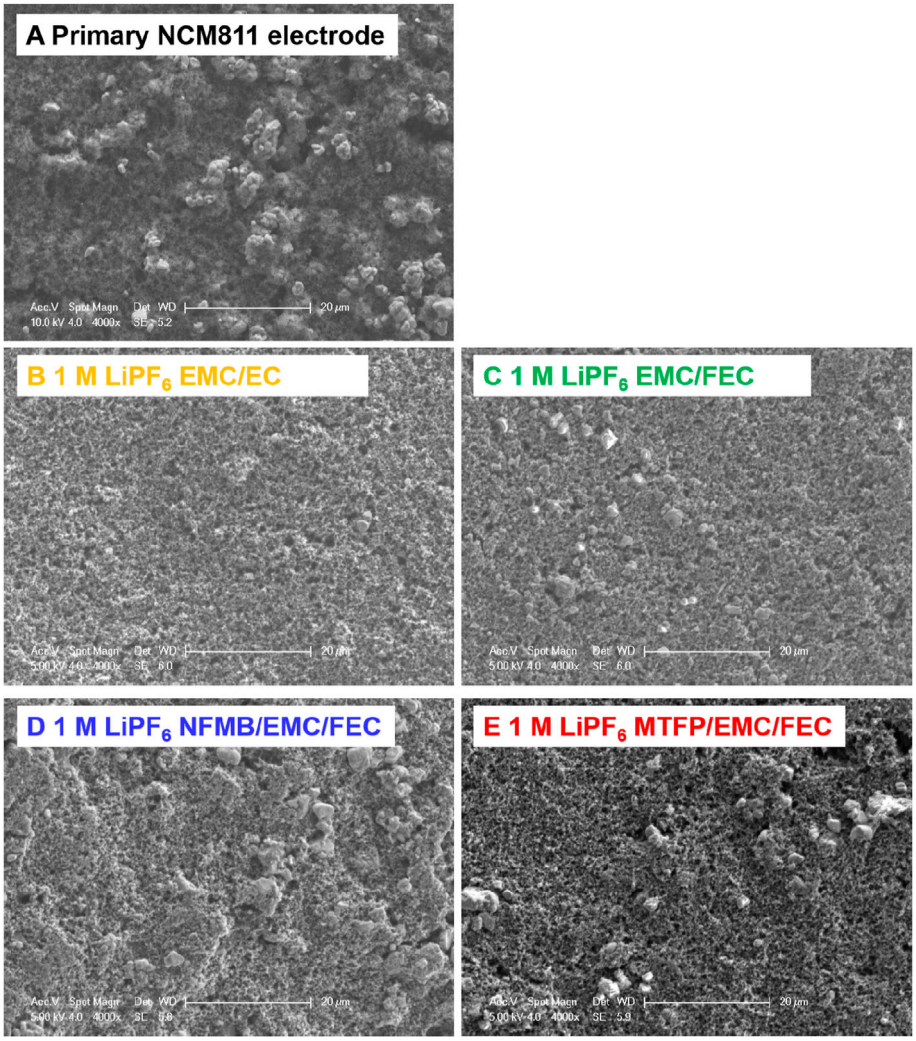

FIGURE 9
SEM images of electrodes at different states: **(A)** primary NCM811 electrode and cycled NCM811 electrode at a cut-off voltage of 2.7–4.8 V after 50 cycles with different electrolyte solutions: **(B)** 1 M LiPF6 EMC/EC, **(C)** 1 M LiPF6 EMC/FEC, **(D)** 1 M LiPF6 NFMB/EMC/FEC, **(E)** 1 M LiPF6 MTFP/EMC/FEC.

discharge capacity of 187.3 mAh g^{-1} at C/8, 172.5 mAh g^{-1} at C/4, 157.9 mAh g^{-1} at C/2, 146.6 mAh g^{-1} at C and 126.7 mAh g^{-1} at 2C, suggesting a poor rate performance. However, the Li/NCM811 cells using the fluorinated solvent-containing electrolytes show a good rate property. Specially, the cells with 1 M $LiPF_6$ NFMB/EMC/FEC show an enhanced rate performance, and deliver a specific capacity of 191.1 mAh g^{-1} at C/8, 177.9 mAh g^{-1} at C/4, 164.6 mAh g^{-1} at C/2, 156 mAh g^{-1} at C. Even at 2C, the discharge capacity can reach to 139 mAh g^{-1}. However, at 4C, the introduction of NFMB and MTFP into the 1 M $LiPF_6$ EMC/FEC electrolyte reduces the reversible capacity of the cells. The reason may be high viscosity of the 1 M $LiPF_6$ NFMB/EMC/FEC and 1M $LiPF_6$ MTFP/EMC/FEC, which cause their low conductivities at room temperature, as shown in Figure 2. When the rate is recovered to C/8, cells using the EC-based electrolyte show a low-capacity retention of 89.54% after 30 cycles, while the cells using 1 M $LiPF_6$ MTFP/EMC/FEC, 1 M $LiPF_6$ NFMB/EMC/FEC and 1 M $LiPF_6$ EMC/FEC display an improved capacity retention of 93.86, 93.62 and 94.37% after 30 cycles, respectively. These data show that the addition of fluorinated co-solvents into the electrolyte can significantly improve the rate performance of the battery, which may be attributed to the interfacial stability of the battery.

The battery with NFMB/EMC/FEC demonstrated better rate performance than that with MTFP/EMC/FEC, however, according to the charge-discharge performances, the cells with MTFP/EMC/FEC showed better cycling stability than that with NFMB/EMC/FEC, especially at high voltage operation.

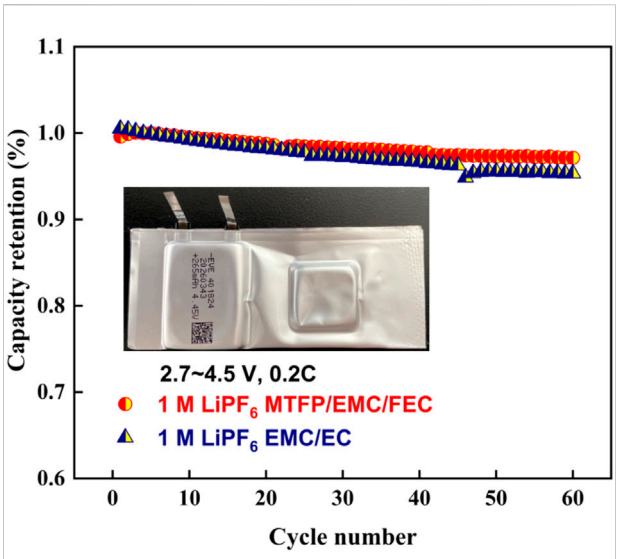

FIGURE 10
Cycling performances of the pouch cells assembled with the 1 M $LiPF_6$ EMC/EC electrolyte and the 1 M $LiPF_6$ MTFP/EMC/FEC electrolyte at room temperature at the rate of 0.2 C.

Therefore, the low-temperature performances were measured to demonstrate the Li^+ transport capability in both the 1 M $LiPF_6$ MTFP/EMC/FEC electrolyte and the 1.0 M $LiPF_6$ EMC/EC electrolyte at a low temperature of −40°C. Figure 7B shows the discharge curves of the coin-cells using these two electrolytes at 0.2 C at 25 and −40°C. The discharge capacities for the fluorinated electrolyte-based cells are 202.2 mAh g^{-1} at 25°C, and 134.7 mAh g^{-1} at −40°C, whereas they are only 180.8 mAh g^{-1} at 25°C, and 109.6 mAh g^{-1} at −40°C for the EC-based cells. Furthermore, the discharge voltage of the cells with 1 M $LiPF_6$ MTFP/EMC/FEC electrolyte is higher than that of the EC-based cells at the corresponding temperature, indicating that the cell with the 1 M $LiPF_6$ MTFP/EMC/FEC electrolyte can deliver a much higher energy output at low temperature of −40°C. The good low temperature of the MTFP-based cells may be due to its higher conductivity at −40°C, which is consistent with the results from the Figure 2.

In order to obtain the NCM811 electrode-electrolyte interface resistance of coin-cells, electrochemical impedance spectroscopy (EIS) was used to measure the impedance change of the battery after 1 cycle and 50 cycle, respectively. As shown in Figure 8A, after the first cycle, the Li/NCM811 cells using the 1 M $LiPF_6$ MTFP/EMC/FEC electrolyte and the 1.0 M $LiPF_6$ NFMB/EMC/FEC electrolyte show a low interfacial impedance, while the cells using the 1.0 M $LiPF_6$ EMC/FEC electrolyte display a high interfacial impedance, suggesting that the introduction of MTFP and NFMB into 1.0 M $LiPF_6$ EMC/FEC, is beneficial to form a low interfacial-impedance interphase on the surface of NCM811 electrodes. Moreover, the values of these interfacial resistance for the cells using fluorinated solvent-containing electrolytes are smaller than that for the cells with the EC-based electrolyte after 1 cycle. In contrast, after 100 cycles, the interfacial resistance at high frequencies on the cycled NCM811 electrodes using both the EC-based electrolyte (1.0 M $LiPF_6$ EMC/EC) and 1.0 M $LiPF_6$ EMC/FEC, is obviously decreased as displayed in Figure 8B. These similar results are consistent with our previous results (Xia et al., 2021), which may be ascribed to the metal ion dissolution from the positive electrodes. For the EIS of 1 M $LiPF_6$ MTFP/EMC/FEC electrolyte, after 50 cycles, this interfacial impedance is slightly decreased in comparison with that after 1 cycle. These results indicated that the interfacial stability has a major impact on the enhancing cycling stability of the cells.

To investigate the interfacial properties of the NCM811 electrodes cycled in different electrolytes, Figure 9 gives the SEM images of the primary NCM811 electrode and cycled NCM811 electrodes at a cut-off voltage of 2.7–4.7 V after 50 cycles. It can be obviously seen from Figure 9A that the SEM image of the primary NCM811 electrode shows some NCM811 micron size-class powder particles. Figure 9B displays that there are nearly no NCM811 particles when cycled in the conventional electrolyte 1.0 M $LiPF_6$ EMC/EC. The reason may be that some degradation species were deposited in the surface of electrode, which is due to the continuous decomposition of the electrolyte 1.0 M $LiPF_6$ EMC/EC at high cut-off potential. In contrast, some NCM811 particles cycled in the fluorinated solvent-containing electrolytes appeared to be well-maintained after 50 cycles (Figures 9D,E). Moreover, the introduction of NFMB and MTFP into the 1 M $LiPF_6$ EMC/FEC electrolyte reduces the excessive growth of the interfacial layer.

To test the compatibility of the prepared electrolyte 1 M $LiPF_6$ MTFP/EMC/FEC with the full battery, Figure 10 compares the cycling performances of the Graphite/$LiCoO_2$ pouch cells with the 1 M $LiPF_6$ MTFP/EMC/FEC electrolyte to those with the conventional electrolyte 1.0 M $LiPF_6$ EMC/EC. As displayed in Figure 10, the pouch cells using the 1 M $LiPF_6$ MTFP/EMC/FEC electrolyte deliver a 97.2% capacity retention after 60 cycles, which is slightly higher than that of the pouch cell with the EC-based electrolyte (95.3%). This result may be attribute to the better anti-oxidative property of the 1 M $LiPF_6$ MTFP/EMC/FEC electrolyte than that of the EC-based electrolyte. These results suggest the good compatibility with the MTFP-based fluorinated electrolyte with two electrodes and low interfacial resistance.

Conclusion

In conclusion, to improve high voltage cycling performance of NCM811 electrodes, we selected the MTFP and NFMB, as a cosolvent for the FEC-based electrolyte. These results showed

that the introduction of MTFP into the electrolyte had excellent high voltage cycling stabilities. Even charged to 4.8 V, the NCM811 cells with 1 M $LiPF_6$ MTFP/EMC/FEC still showed excellent performance. After 100 cycles, the discharge capacity still reached to 183.9 mAh g^{-1}, that is, 93.4% capacity retention of its second capacity. We infer that the interfacial stability has a major impact on the enhancing cycling stability of the cells.

Data availability statement

The original contributions presented in the study are included in the article/Supplementary material, further inquiries can be directed to the corresponding author.

Author contributions

MC did most experiments and wrote the first draft of the manuscript. RZ performed some experiments. LX supervised the work, modified, and edited the manuscript. All authors contributed to manuscript revision, read, and approved the submitted version.

Funding

This work is supported by the National Natural Science Foundation of China (no. 22075155), the Ningbo Science and Technology Innovation 2025 Major Project (no. 2021Z121), and the Zhejiang Provincial Natural Science Foundation of China (no. LY19B030004).

Conflict of interest

RZ was employed by the company EVE Energy Co., Ltd.

The remaining authors declare that the research was conducted in the absence of any commercial or financial relationships that could be construed as a potential conflict of interest.

Publisher's note

References

Cao, X., Ren, X., Zou, L., Engelhard, M. H., Huang, W., Wang, H., et al. (2019a). Monolithic solid–electrolyte interphases formed in fluorinated orthoformate-based electrolytes minimize Li depletion and pulverization. *Nat. Energy* 4 (9), 796–805. doi:10.1038/s41560-019-0464-5

Cao, X., Xu, Y., Zhang, L., Engelhard, M. H., Zhong, L., Ren, X., et al. (2019b). Nonflammable electrolytes for lithium ion batteries enabled by ultra-conformal passivation interphases. *ACS Energy Lett.* 4 (10), 2529–2534. doi:10.1021/acsenergylett.9b01926

Chen, M., Zhao, E., Chen, D., Wu, M., Han, S., Huang, Q., et al. (2017). Decreasing Li/Ni disorder and improving the electrochemical performances of Ni-rich $LiNi_{0.8}Co_{0.1}Mn_{0.1}O_2$ by Ca doping. *Inorg. Chem.* 56 (14), 8355–8362. doi:10.1021/acs.inorgchem.7b01035

Fan, X., Chen, L., Borodin, O., Ji, X., Chen, J., Hou, S., et al. (2018). Non-flammable electrolyte enables Li-metal batteries with aggressive cathode chemistries. *Nat. Nanotechnol.* 13 (8), 715–722. doi:10.1038/s41565-018-0183-2

Fan, X., and Wang, C. (2021). High-voltage liquid electrolytes for Li batteries: progress and perspectives. *Chem. Soc. Rev.* 50, 10486–10566. doi:10.1039/d1cs00450f

Fan, X., Xiao, J., Chen, L., Chen, J., Deng, T., Han, F., et al. (2019). All-temperature batteries enabled by fluorinated electrolytes with non-polar solvents. *Nat. Energy* 4 (10), 882–890. doi:10.1038/s41560-019-0474-3

Gu, W., Xue, G., Dong, Q., Yi, R., Mao, Y., Zheng, L., et al. (2022). Trimethoxyboroxine as an electrolyte additive to enhance the 4.5 V cycling performance of a Ni-rich layered oxide cathode. *eScience*. doi:10.1016/j.esci.2022.05.003

Guan, D., Hu, G., Peng, Z., Cao, Y., Wu, J., Huang, M., et al. (2022). A nonflammable low-concentration electrolyte for lithium-ion batteries. *J. Mat. Chem. A* 10, 12575–12587. doi:10.1039/D2TA01760A

He, W., Guo, W., Wu, H., Lin, L., Liu, Q., Han, X., et al. (2021). Challenges and recent advances in high capacity Li-rich cathode materials for high energy density lithium-ion batteries. *Adv. Mat.* 33 (50), e2005937. doi:10.1002/adma.202005937

Heist, A., Hafner, S., and Lee, S. H. (2019). High-energy nickel-rich layered cathode stabilized by ionic liquid electrolyte. *J. Electrochem. Soc.* 166 (6), A873–A879. doi:10.1149/2.0071906jes

Huang, Y., Yao, X., Hu, X., Han, Q., Wang, S., Ding, L.-X., et al. (2019). Surface coating with Li-Ti-O to improve the electrochemical performance of Ni-rich cathode material. *Appl. Surf. Sci.* 489, 913–921. doi:10.1016/j.apsusc.2019.06.012

Lan, G., Zhou, H., Xing, L., Chen, J., Li, Z., Guo, R., et al. (2019). Insight into the interaction between Ni-rich $LiNi_{0.8}Co_{0.1}Mn_{0.1}O_2$ cathode and BF_4− introducing electrolyte at 4.5 V high voltage. *J. Energy Chem.* 39, 235–243. doi:10.1016/j.jechem.2019.04.011

Leach, A. S., Llewellyn, A. V., Xu, C., Tan, C., Heenan, T. M. M., Dimitrijevic, A., et al. (2022). Spatially resolved operando synchrotron-based X-ray diffraction measurements of Ni-rich cathodes for Li-ion batteries. *Front. Chem. Eng.* 3, 794194. doi:10.3389/fceng.2021.794194

Lee, Y., Lee, T. K., Kim, S., Lee, J., Ahn, Y., Kim, K., et al. (2019). Fluorine-incorporated interface enhances cycling stability of lithium metal batteries with Ni-rich NCM cathodes. *Nano Energy* 67, 104309. doi:10.1016/j.nanoen.2019.104309

Li, J., Downie, L. E., Ma, L., Qiu, W., and Dahn, J. R. (2015). Study of the failure mechanisms of $LiNi_{0.8}Co_{0.1}Mn_{0.1}O_2$ cathode material for lithium ion batteries. *J. Electrochem. Soc.* 162 (7), A1401–A1408. doi:10.1149/2.1011507jes

Li, J., Liu, H., Xia, J., Cameron, A. R., Nie, M., Botton, G. A., et al. (2017). The impact of electrolyte additives and upper cut-off voltage on the formation of a rocksalt surface layer in $LiNi_{0.8}Co_{0.1}Mn_{0.1}O_2$ electrodes. *J. Electrochem. Soc.* 164 (4), A655–A665. doi:10.1149/2.0651704jes

Li, L., Fu, L., Li, M., Wang, C., Zhao, Z., Xie, S., et al. (2022). B-doped and La_4NiLiO_8-coated Ni-rich cathode with enhanced structural and interfacial stability for lithium-ion batteries. *J. Energy Chem.* 71, 588–594. doi:10.1016/j.jechem.2022.04.037

Li, W., Erickson, E. M., and Manthiram, A. (2020). High-nickel layered oxide cathodes for lithium-based automotive batteries. *Nat. Energy* 5 (1), 26–34. doi:10.1038/s41560-019-0513-0

Lim, B. B., Myung, S. T., Yoon, C. S., and Sun, Y. K. (2016). Comparative study of Ni-rich layered cathodes for rechargeable lithium batteries: $Li[Ni_{0.85}Co_{0.11}Al_{0.04}]O_2$ and $Li[Ni_{0.84}Co_{0.06}Mn_{0.09}Al_{0.01}]O_2$ with two-step full concentration gradients. *ACS Energy Lett.* 1 (1), 283–289. doi:10.1021/acsenergylett.6b00150

Lim, S. H., Jung, K., Lee, K., Mun, J., Han, Y., and Yim, T. (2020). Triethanolamine borate as a surface stabilizing bifunctional additive for Ni-rich layered oxide cathode. *Int. J. Energy Res.* 45 (2), 2138–2147. doi:10.1002/er.5907

Liu, L., Gao, W., Cui, Y., and Chen, S. (2019). A bifunctional additive bi(4-flurorophenyl) sulfone for enhancing the stability and safety of nickel-rich cathode based cells. *J. Alloys Compd.* 820, 153069. doi:10.1016/j.jallcom.2019.153069

Liu, X., Mariani, A., Diemant, T., Pietro, M. E. D., Dong, X., Kuenzel, M., et al. (2022). Difluorobenzene-based locally concentrated ionic liquid electrolyte enabling stable cycling of lithium metal batteries with nickel-rich cathode. *Adv. Energy Mat.* 12, 2200862. doi:10.1002/aenm.202200862

Niu, C., Liu, D., Lochala, J. A., Anderson, C. S., Cao, X., Gross, M. E., et al. (2021). Balancing interfacial reactions to achieve long cycle life in high-energy lithium metal batteries. *Nat. Energy* 6 (7), 723–732. doi:10.1038/s41560-021-00852-3

Park, K. J., Lim, B. B., Choi, M. H., Sun, Y. K., Haro, M., Vicente, N., et al. (2015). High-capacity $Li[Ni_{0.8}Co_{0.06}Mn_{0.14}]O_2$ positive electrode with a dual concentration gradient for next-generation lithium-ion batteries. *J. Mat. Chem. A Mat.* 3, 22183–22190. doi:10.1039/c5ta05657h

Pham, H. Q., Hwang, E. H., Kwon, Y. G., and Song, S. W. (2019). Approaching the maximum capacity of nickel-rich $LiNi_{0.8}Co_{0.1}Mn_{0.1}O_2$ cathodes by charging to high-voltage in a non-flammable electrolyte of propylene carbonate and fluorinated linear carbonates. *Chem. Commun.* 55 (9), 1256–1258. doi:10.1039/c8cc10017a

Ryu, H. H., Park, K. J., Yoon, C. S., and Sun, Y. K. (2018). Capacity fading of Ni-rich $Li[Ni_xCo_yMn_{1-x-y}]O_2$ ($0.6 \leq x \leq 0.95$) cathodes for high-energy-density lithium-ion batteries: Bulk or surface degradation? *Chem. Mat.* 30 (3), 1155–1163. doi:10.1021/acs.chemmater.7b05269

Schipper, F., Bouzaglo, H., Dixit, M., Erickson, E. M., Weigel, T., Talianker, M., et al. (2017). From surface ZrO_2 coating to bulk Zr doping by high temperature annealing of nickel-rich lithiated oxides and their enhanced electrochemical performance in lithium ion batteries. *Adv. Energy Mat.* 8 (4), 1701682. doi:10.1002/aenm.201701682

Wang, X., Salari, M., Jiang, D., Chapman Varela, J., Anasori, B., Wesolowski, D. J., et al. (2020). Electrode material–ionic liquid coupling for electrochemical energy storage. *Nat. Rev. Mat.* 5, 787–808. doi:10.1038/s41578-020-0218-9

Xia, L., Miao, H., Wang, F., Zhang, C., Wang, J., Zhao, J., et al. (2021). Investigation of fluorinated ether-containing electrolytes for high energy-density nickel-rich $LiNi_{0.8}Co_{0.1}Mn_{0.1}O_2$ electrodes. *Int. J. Energy Res.* 45 (7), 9936–9947. doi:10.1002/er.6488

Xu, G., Liu, X., Daali, A., Amine, R., Chen, Z., and Amine, K. (2020). Challenges and strategies to advance high-energy nickel-rich layered lithium transition metal oxide cathodes for harsh operation. *Adv. Funct. Mat.* 30 (46), 2004748. doi:10.1002/adfm.202004748

Xue, W., Huang, M., Li, Y., Zhu, Y. G., Gao, R., Xiao, X., et al. (2021). Ultra-high-voltage Ni-rich layered cathodes in practical Li metal batteries enabled by a sulfonamide-based electrolyte. *Nat. Energy* 6 (5), 495–505. doi:10.1038/s41560-021-00792-y

Yang, S., Lin, J., Zhang, Z., Zhang, C., Zheng, X., Xie, W., et al. (2022). Advanced engineering materials for enhancing thermal management and thermal safety of lithium-ion batteries: A review. *Front. Energy Res.* 10, 949760. doi:10.3389/fenrg.2022.949760

Zhang, X., Zou, L., Cui, Z., Jia, H., Engelhard, M. H., Matthews, B. E., et al. (2021). Stabilizing ultrahigh-nickel layered oxide cathodes for high-voltage lithium metal batteries. *Mat. TodayKidlingt.* 44, 15–24. doi:10.1016/j.mattod.2021.01.013

Zhu, C., Sun, C., Li, R., Weng, S., Fan, L., Wang, X., et al. (2022). Anion–diluent pairing for stable high-energy Li metal batteries. *ACS Energy Lett.* 7 (4), 1338–1347. doi:10.1021/acsenergylett.2c00232